Evaluation of TiO_2 derived mesoporous spherical photocalysts for the oxidation of industrial waste water treatment process

Tae-Ho Yoon[*], Kyung-Han Ko, Myung-Han Ko, and Summook Lee

Abstract — **This paper mainly discussed the performance of photocatalysts which are prepared cation exchange resin and TiCl₃ precursor via heat treatment process to enhance their photocatalytic potentials. The morphology and size of TiO_2 photocatalyst was well ordered spherical shape and average diameter of 0.30 ~0.45 mm with well dispersed by TiO_2 on the surface of spherical activated carbon. TiO_2 supported on spherical activated carbon contains two different phases; anatase (83%) and rutile (17%). The TiO_2 photocatalyst had high specific surface area of 1,649 m^2/g and high total pore volume of 1.61 cm^3/g. Adsorption characteristics and photocatalytic activity of TiO_2 photocatalyst were evaluated by the removal of humic acid from waste water model aqueous solution. Catalyst dosage, initial humic acid concentration, and coexisting ions have influences on the photocatalytic degradation of humic acid. The degradation of humic acid by meso-TiO2/SAC was dependent on catalyst dosage, initial its concentration. TiO_2 photocatalyst has potentials for application as adsorbent and also as a photocatalyst in the removal of humic acid from groundwater and surface water.**

Keywords —**photocatalysts, degradation of organic compound, nano porous materials, waste water treatment**

I. Introduction

Industrial wastewater is of global concern due to its severe effects on the environment. Compared with municipal wastewater, industrial wastewater generally contains high concentration of toxic or non-biodegradable pollutants, such as fats, oil, grease, heavy metals, phenols, and ammonia[1]. Therefore, advanced oxidation processes (AOPs), which rely on the generation of highly reactive and oxidizing hydroxyl radicals (·OH), are considered as highly competitive water treatment technologies[2].

As an important technology of AOPs, photocatalytic oxidation (PCO) has attracted increasing attention in recent

*Tae-Ho Yoon, Ph.D. (Corresponding author)
Electronics and Telecommunications Research Institute (ETRI)
South Korea

Kyung-Han Ko
CTOC Materials Co. LTD.
South Korea

Myung-Han Ko, Ph.D.
ANT21 Co. LTD.
South Korea

Sunmook Lee, Ph.D.
Korea Conformity Laboratories (KCL)

years because of its excellent performance on pollutants removal, low cost, and photochemical stability and without addition of toxic chemicals [3, 4]. Titanium dioxide(TiO_2) is widely used as a photo catalysts which degrade hydrocarbon under the existence of ultraviolet or increase of hydrophilicity of surface for self-cleaning effect in the fields of surface chemistry as bulk film coating in heterogeneous photo catalysts, because of its photo-stability, nontoxicity, low cost, and stability in water under most environmental conditions [5-7]. By these advantages, PCO has attracted increasing attention in recent years because of its excellent performance on pollutants removal, low cost, and photochemical stability and without addition of toxic chemicals [8, 9].

Large amount of reactive oxygen species such as hydroxyl radicals (·OH) and superoxide radical anion (·O₂) are produced on the surface of TiO_2 under UV light irradiation, and these reactive radicals are regarded as the major responsible species for the degradation of organic pollutants in wastewater [7–8]. The results revealed that the wastewater quality characteristics have obvious influence on the photo-degradation rate of the pollutants. PCO can also serve as a pretreatment, which can significantly enhance the biodegradability of industrial wastewater to meet requirements of the subsequent bio-treatment process[9, 10].

This paper deals with the characterization of photocatalyst prepared conveniently with ion exchange precursor and titanium precursor and heat-treatment process. To evaluate the performance of prepared photocatalysts, humic acid was chosen as a pollutant to be removed by adsorption and photocatalytic degradation using TiO_2 photocatalysts. Humic acid mostly consists of natural organic matter, it is non-biodegradable and has color (undesirable color at concentration above 5 mg/L), odor and also exhibits a wide range of distribution in molecular weight and size[11, 12]. For this work, we prepared in-house PCO device with 2L of working volume capacity.

II. Materials and Methods

A. *Materials*

To prepare photocatalyst, cation ion-exchange resin (SAIR, Diaion SK1BH, Samyang Co. Ltd., South Korea), with a diameter range of 0.4–0.5 mm average particle size, was used as a support of the TiO_2 photocatalyst. Titanium trichloride (TiCl₃, 20%, Kanto Chemical, Japan) as a Ti precursor was used without any additional purification process. Commercial TiO_2 powder P25(Degussa Chemical, Germany) used as a reference. Humic acid was purchased from Aldrich Chemical Company, which has carbon, hydrogen, and nitrogen content of 39.44%, 4.74%, and

0.79%, respectively. Distilled water was used in all the experiments.

B. *Preparation of TiO₂ photocatalyst*

The TiO₂ photocatalysts was prepared via a previously described ion exchange method and heat-treatment process [13,14]. Titanium trichloride, distilled water and ion-exchange resin were mixed in a weight ratio of $TiCl_3:H_2O:SK1BH = 1:30:12$ and then stirred at 150 rpm for 1 hr at ambient temperature. The ion-exchange resin containing Ti was rinsed severally with distilled water until pH reached 7.0, then it is dried at 110 ℃ for 24 hrs in an oven. Stabilization process is performed at 300 ℃ for 5 h under atmospheric condition with a heating rate of 1 ℃/min. The stabilized sample was carbonized at 700 ℃ for 10 min under a nitrogen conditions with flow rate of 2 L/min with a heating rate of 3 ℃/min and also activated under a nitrogen/steam at 900 ℃ for 570 min. The heating rate was 1 ℃/min up to 900 ∘C.

C. *Characterization of TiO₂ photocatalyst*

The surface morphology and size TiO₂ photocatalyst was observed using scanning electron microscopy (SEM, JSM-6700F, JEOL), and the detailed microstructure of meso-TiO2/SAC was examined by field emission transmission electron microscopy (FE-TEM, Tecnai F20, FEI Co.). The crystalline phase of TiO₂ photocatalyst was identified by X-ray diffractometer (XRD, D/MAX-IIIB, Rigaku) employing Cu K_α radiation and operating at 2.0 kW with scanning speed of 5∘/min over the 2θ range 20–80∘. The specific surface area and pore structure of TiO₂ photocatalyst was determined from nitrogen adsorption–desorption isotherm at 77 K (ASAP 2010, Micromeritics Company). The specific surface area was determined by Brunauer–Emmett–Teller (BET) method and pore size distribution was analyzed using the Barrett–Joyner–Halenda (BJH) method.

D. *Adsorption isotherm estimation*

Model solution of humic acid was prepared with different concentrations of 20~100 ppm by dissolving into distilled water. The solution was stirred for 24 hrs and filtered through membrane filter (0.45 μm). For the equilibrium experiments, 1.8 g of TiO₂ were added into 200 mL of different initial concentrations of humic acid solutions. The solutions were stirred using a shaker with 25 ℃ and 150 rpm and kept under dark conditions for 10 h. The amount of humic acid adsorbed by TiO₂, q_t (mg/g) at each time interval was calculated by following equations;

$$q_t(mg \ / g) = (C_0 - C_t)\frac{V}{m} \qquad (1)$$

Where, C_0 : the initial concentration of humic acid (mg/L),

C_t : the remaining concentration of humic acid at certain time (mg/L), respectively.

V : the volume of the humic acid solution (L)

m : the amount of TiO₂ used in experiments(g)

E. *Photocatalytic degradation experiments*

Batch photocatalytic reaction had been performed in the 2 L working volume of fluidized bed photo oxidation reactor, which was made of stainless steel (10 cm diameter, 40 cm height). A schematic diagram of the photocatalytic reactor is shown in Fig. 1. Low pressure mercury lamp (UV-C, max = 254 nm, G18T5C, Light tech) used as a light source was located at the center of the reactor. 20 mg/L humic acid and appropriate amount of TiO₂ put into the reactor and then air was bubbled to reaction solution through the bottom of the reactor with an air flow of 200 mL/min to help reaction and floating of catalyst. Prior to photocatalytic experiment, sample was stirred in the dark for 10 h to reach an adsorption–desorption equilibrium. After stirring for 10 h, concentration of humic acid was noted C_0.
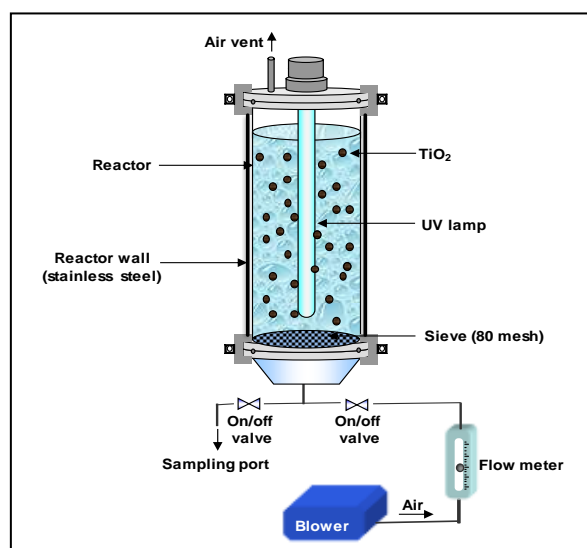

Figure 1.   Schematic diagram of photocatalytic reaction experimental setup.

Every sample was collected by regular intervals for the analysis of residual humic acid concentration. To examine the effect of catalyst dosage on the photocatalytic experiment, dosage of TiO₂ was varied from 6 to 12 g/L. The stability of photocatalyst was assessed through repeated use of TiO₂. Repeat experiments were carried out with 20 mg/L humic acid concentration, 9 g/L photocatalyst, and 10 h UV irradiation for cycling run. After the first photocatalytic reaction, remaining solution was replaced with fresh HA solution of 20 mg/L. The used TiO₂ was rinsed 5 times with distilled water for the next cycles. The above procedure was repeated for seven cycles. Blank experiments were conducted under the same conditions without photocatalyst. To compare with commercially available P25, TiO₂, photocatalyst was applied as a reference. In the photocatalytic experiment using P25 TiO₂, collected samples after photocatalysis were centrifuged at 13,000 rpm for 15 min to separate P25 TiO2 particles from sample solution before TOC analysis. The degradation efficiency (%) of humic acid was calculated by Eq. (2), where C_0 and C_t are the equilibrium concentration of humic acid after adsorption and the remaining concentration of HA at certain time, respectively.

The concentration of humic acid was determined by UV-vis spectrophotometer (Qvis 4000, Cmac). The mineralization degree was assessed by total organic carbon (TOC) analysis, performed on a TOC analyzer (Torch,

Teledyne Tekmar). Chemical oxygen demand(COD) was also measured using COD test kit (Cmac).

$$Degradation\ efficiency(\%) = \left(\frac{C_0 - C_t}{C_0} \right) \times 100 \qquad (2)$$

III. Results

A. Characterization of TiO₂ photocatalyst

As shown in figure 2(a), SEM image of TiO₂ shows good spherical shape with smooth surface without any defects and average diameter photocatalysts observed under SEM was in the range of 0.30 ~ 0.45 mm with narrow size distribution. It implies that TiO₂ can be easily separated from the treated solution after the photocatalytic reaction due to their relatively large diameter compare than that of nano size of P25 photocatalysts. FE-TEM was used to obtain more detailed microstructure information and the result is presented in figure 2(b). It can be clearly seen that the TiO2 with ranging 10–30 nm was relatively well dispersed over the surface of spherical activated carbon.
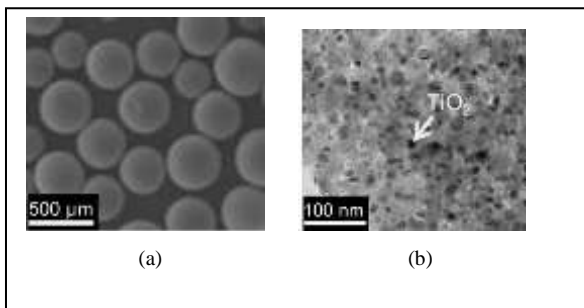

(a)   (b)

Figure 2. (a) SEM image of prepared TiO₂ photocatalytsts and (b) FE-TEM image of TiO₂ photocatalytsts.

To evaluate the crystalline structure of TiO₂, XRD analysis was performed and showed results in figure 3. XRD pattern of P25 TiO₂ was also presented. It can be seen that peak positions of TiO₂ were similar with P25 TiO₂ and exhibited mixture of anatase/rutile phases. The relative content of anatase and rutile was estimated using Spurr–Myers equation, $A(\%) = (IA/IA + 1.265IR) \times 100$, where A (%) is the relative content of anatase, IA and IR are the intensities of the anatase (101) peak at $2\theta = 25.2°$ and the rutile (110) peak at $2\theta = 27.3°$. The TiO₂ has a relative content of 83% for anatase and 17% for rutile. Degussa P25 TiO₂, which is well known to have high photocatalytic activity, consists 78% anatase and 22% rutile. Ratio of anatase and rutile for meso-TiO2/SAC looks quite similar to that of P25 TiO₂. A mixture of anatase/rutile also exhibits a higher photocatalytic activity than that of each of the pure phases.

To measure the specific surface area of TiO₂ photocatalyst, BET measurement was performed. The specific surface area of TiO₂ photocatalyst was found to be 1,649 m²/g (ca. 30 times higher than that of the Degussa P25 TiO₂). This value is similar with the most widely used commercial activated carbon, (800–1500 m²/g). The nitrogen adsorption–desorption isotherm of TiO₂

photocatalyst is presented in figure 4. The isotherm exhibits a typical IUPAC type IV with a hysteresis loop at high relative pressure of P/P₀ = 0.6–1.0, thus indicating the presence of mesopores. The ranges of pores were located at 0.8–35 nm. It was observed that TiO₂ photocatalysts showed a bimodal pore size distribution, that is, micropores with ranging from 1 nm to 1.6 nm and mesopores in the range of 5–20 nm. The average pore size of TiO₂ photocatalyst was 8.39 nm, suggesting that mesopores in TiO₂ photocatalyst are more dominant.
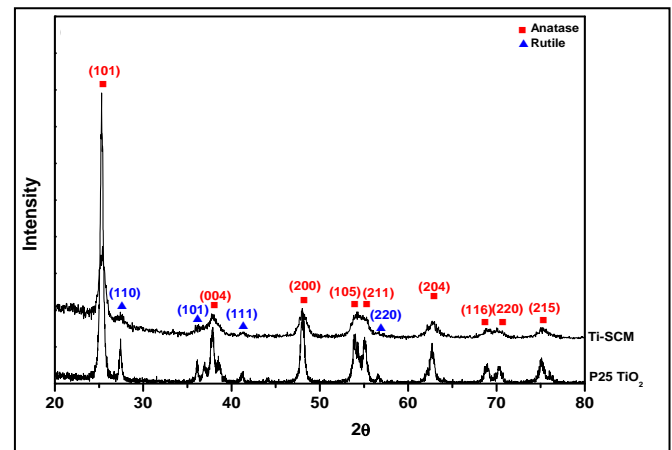

Figure 3. Comparison of XRD pattern between TiO₂ photocatalyst prepared from cation exchange resin with TiCl₃ and commercial P25 TiO₂.

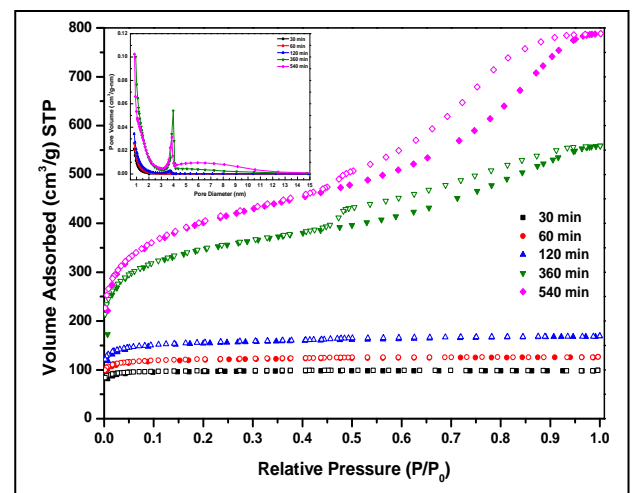
Figure 4. Nitrogen adsorption–desorption isotherm of TiO₂. Inset: pore size distribution of the isotherm for TiO₂ photocatalysts depending on the pyrolysis time.

B. Adsorption properties of photocatalysts

In order to evaluate adsorption characteristics of humic acid on TiO₂ photocatalyst, adsorption kinetics was performed in the dark conditions varying initial concentration of humic acid in the range of 20–100 mg/L as shown in figure 5. It was found that adsorption of humic acid on TiO₂ photocatalyst occurred despite that humic acid has large molecular size and equilibrium adsorption was reached almost in about 2 hrs. Spherical activated carbon has large number of adsorption sites because of their

developed well pore structure with very large surface area. This may be supported by the existence of mesopores (pore size: 5–20 nm) of TiO_2 photocatalyst, as shown in inset of figure 4.
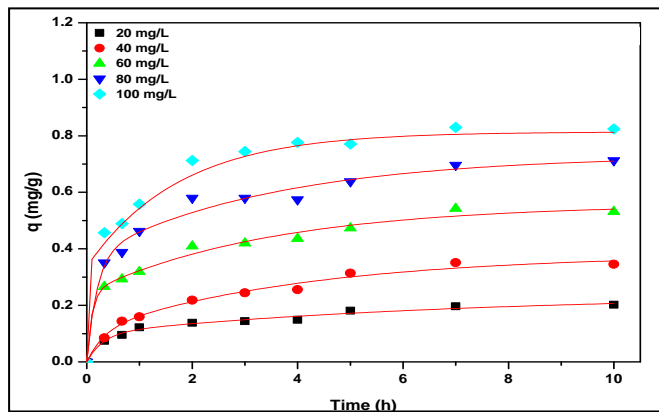

Figure 5. Adsorption kinetics of humic acid TiO_2 photocatalyst at various initial concentrations (catalyst dosage = 9 g/L, pH 7.4).

C. *Photocatalytic degradation experiments*

To evaluate effect of catalyst amounts, photocatalytic experiments were conducted with varying catalyst dosage from 6 to 12 g/L, and the results obtained were shown in figure 6. Mineralization degree of humic acid was enhanced from 60 to 80% with the increase of catalyst dosage from 6 to 9 g/L. However, TOC removal efficiency was constant when catalyst dosage was beyond 9 g/L. Increase in catalyst dosage contributes to increased number of active sites but may reduce the degradation efficiency of humic acid by blocking UV irradiation. It can be said that about a 9 g/L dosage is suitable for practical applications from the economic point of view.
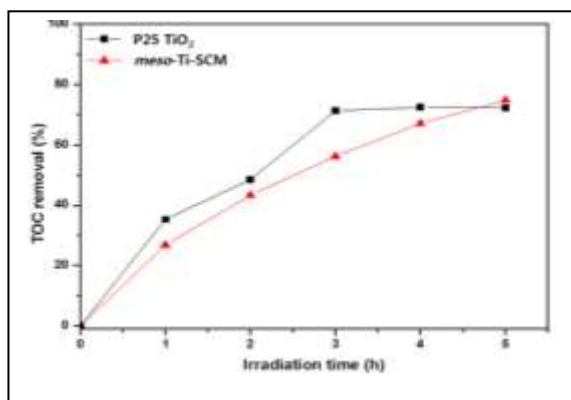

Figure 6. Effect of catalyst dosage on the photocatalytic degradation of humic acid by TiO_2 photocatalyst ([Humic acid]$_0$ = 20 mg/L, pH 7.4, irradiation time = 10 h).

Photocatalytic experiment was carried out to assess the efficiency of TiO_2 photocatalyst at different initial concentrations of humic acid in the range 20 ~100 mg/L since the initial concentration of pollutant is a very important parameter in water treatment. Figure 7(a) shows that the degradation efficiency of humic acid by TiO_2 photocatalyst greatly decreased with increase in initial concentration of humic acid from 20 to 100 mg/L.

Equilibrium concentration of TOC after reaching an adsorption–desorption equilibrium was 18.2, 45.8, and 92.5 mg/L for 20, 50 and 100 mg/L of initial HA concentration, respectively. The kinetics of HA degradation by meso-TiO2/SAC was analyzed using a first-order kinetic expressed in Eq. (3)

$$\ln\left(\frac{[TOC]_0}{[TOC]_t}\right) = kt \qquad (3)$$

Where, $[TOC]_0$: equilibrium concentration of TOC after adsorption in the dark,

$[TOC]_t$: remaining concentration of TOC at irradiation time t,

k : rate constant of first-order,
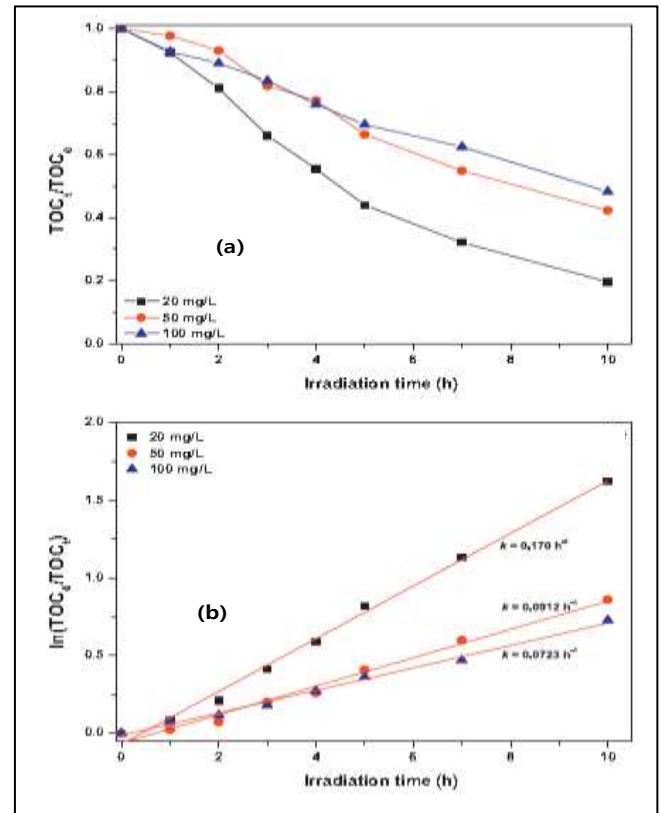
t : irradiation time

Figure 7. (a) TOC change and (b) first-order kinetics of the photocatalytic degradation of humic acid at different initial concentrations (catalyst dosage = 9 g/L, pH 7.4).

Figure 7(b) is the plots of $\ln([TOC]_0/[TOC]_t)$ versus t. All the curves showed arranged well linear correlation (R^2 > 0.993), suggesting that the degradation of humic acid by TiO_2 photocatalysts followed a first-order kinetic. The k obtained from slope of the plots was 0.170, 0.0912, and 0.0723 h^{-1} for 20, 50, and 100 mg/L, respectively. The rate constants of TOC removal decreased with increasing initial humic acid concentration in the model solution. When the humic acid concentration increase, more humic acid molecules covering the photocatalytical active site of TiO_2 photocatalyst. Thus, a number of photons which interacts with these sites decrease. As a result, hydroxyl radicals generation decrease, degradation rate of humic acid also decrease.
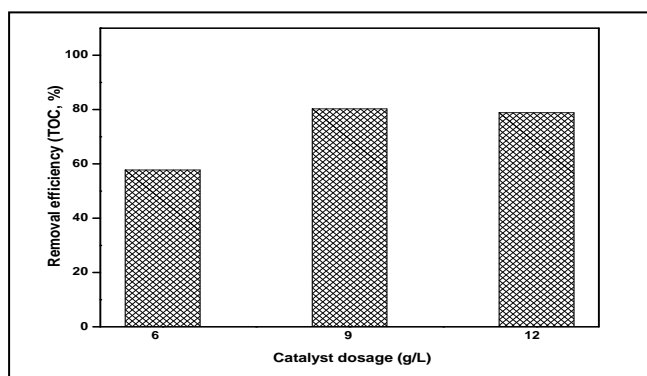
Figure 8. Comparison of P25 TiO_2 and TiO_2 photocatalyst on the photocatalytic degradation of humic acid ($[humic\ acid]_0 = 20$ mg/L, catalyst dosage = 9 g/L (TiO_2 photocatalyst), 0.4 g/L (P25 TiO_2), pH 7.4).

To compare the photocatalytic efficiency between prepared TiO_2 photocatalyst and commercial photocatalysts P25 TiO_2, photocatalytic experiment was conducted for 20 mg/L humic acid using P25 TiO_2 of 0.4 g/L. At that time, the amount of P25 TiO_2 corresponds to the titanium content (3 wt%) of 9 g/L of TiO_2 photocatalyst. It was observed that degradation efficiency of humic acid was about 77% after UV irradiation for 5 h as shown in figure 8. It was similar with that of TiO_2 photocatalysts. Moreover, different from P25 TiO_2, prepared TiO_2 photocatalyst could be easily separated from aqueous solution after use, and also the intermediates produced during photocatalytic degradation of humic acid can be also adsorbed by activated carbon and then further oxidized to avoid the secondary pollution caused by the intermediates. Also, TiO_2 photocatalyst may be beneficial over P25 TiO_2 for application to continuous flow systems and in the fluidized bed photoreactor system.

IV. **Conclusions**

The TiO_2 photocatalyst prepared from cation exchange resin and $TiCl_3$ precursor and heat treatment process was studied for its photocatalytic potentials. The morphology and size of TiO_2 photocatalyst observed by the SEM analysis was smooth spherical shape and diameter of 0.30 ~0.45 mm. The TEM analysis showed that the TiO_2 was well dispersed on the surface of spherical activated carbon and the XRD analysis was confirmed that TiO_2 supported on spherical activated carbon contain two different phases; anatase (83%) and rutile (17%). The TiO_2 photocatalyst had high specific surface area of 1,649 m^2/g and high total pore volume of 1.61 cm^3/g. It was observed that the pore size distribution curve had two distinct portions with peak pore of ca. 1.3 nm and 10 nm. The pore diameter of the majority of mesopores was in the range 5~ 20 nm. Adsorption characteristics and photocatalytic activity of TiO_2 photocatalyst were evaluated by the removal of humic acid from waste water model aqueous solution. It was discovered that the adsorption equilibrium of humic acid on TiO_2 photocatalyst was reached in about 2 hrs. Catalyst dosage, initial humic acid concentration, and coexisting ions have influences on the photocatalytic degradation of humic acid. The degradation of humic acid by meso-TiO2/SAC was dependent on catalyst dosage, initial its concentration. TiO_2 photocatalyst has potentials for application as adsorbent and also as a photocatalyst in the removal of humic acid from groundwater and surface water.

References

[1] N. S. A.Mutamim, Z. Z. Noor,M. A. A. Hassan, and G. Olsson, " Application of membrane bioreactor technology in treating high strength industrial wastewater: a performance review," Desalination, vol. 305, pp. 1–11, 2012.

[2] T. Zhang, X. Wang, and X. Zhang, "Recent progress in TiO_2-mediated solar photocatalysis for industrial wastewater treatment", Int'l J. Photoenergy, vol. 42, pp. 2640-2648, 2008.

[3] M. R. Hoffmann, S. T.Martin,W. Choi, and D.W. Bahnemann, ″Environmental applications of semiconductor photocatalysis," Chemical Reviews, vol. 95, pp. 69–96, 1995.

[4] M. N. Chong, B. Jin, C. W. K. Chow, and C. Saint, "Recent developments in photocatalytic water treatment technology: a review," Water Research, vol. 44, no. 10, pp. 2997–3027, 2010.

[5] J. Shang, W. Li, and Y. F. Zhu, "Structure and photocatalytic characteristics of TiO2 film photocatalyst coated on stainless steel web-net", J. Molecular Catalysis A-Chemical, vol.202, pp.187–195, 2003.

[6] S. S. Madaeni, and N. Ghaemi, "Characterization of self-cleaning RO membranes coated with TiO_2 particles under UV irradiation", J. Membrane Science, vol. 303, pp. 221-218, 2007.

[7] T. Zhang,X.Yan, andD.D. Sun, "Hierarchicallymultifunctional K-OMS-2/TiO2/Fe3O4 heterojunctions for the photocatalytic oxidation of humic acid under solar light irradiation," Journal of Hazardous Materials, vol. 243, pp. 302–310, 2012.

[8] Y.Kuwahara, T.Kamegawa, K.Mori, and H. Yamashita, "Design of new functional Titanium oxide-based photocatalysts for degradation of organics diluted in water and air," Current Organic Chemistry, vol. 14, , pp. 616–629, 2010.

[9] A. Fujishima, T. N. Rao, D. A. Tryk, and J. Photoch, "Titanium dioxide photocatalysis," Journal of Photochemistry and Photobiology C: Photochemistry Reviews, vol. 1, pp. 1–21, 2000.

[10] A. L. Linsebigler, G. Q. Lu, and J. T. Yates Jr., "Photocatalysis on TiO_2 surfaces: principles, mechanisms, and selected results," Chemical Reviews, vol. 95, pp. 735–758, 1995.

[11] A. Imyim, and E. Prapalimrungsi, "Humic acids removal from water by aminopropyl functionalized rice husk ash", J. Hazard. Mater. vol. 184, pp. 775–781, 2010.

[12] Sh. Maghsoodloo, B. Noroozi, A. K. Haghi, and G. A. Sorial, "Consequence of chitosan treating on the adsorption of humic acid by granular activated carbon", J. Hazard. Mater. vol. 191. pp.380–387, 2011.

[13] J. W. Yoon, M. H. Baek, J. S. Hong, C. Y. Lee, J. K. Suh, "Photocatalytic degradation of azo dye using TiO_2 supported on spherical activated carbon", Kor. J. Chem. Eng., vol. 29, pp. 1722-1729, 2012.

[14] H. J. Jung, J. S. Hong, J. K. Suh, "A study on removal efficiency of phenol and humic acid using spherical activated carbon doped by TiO_2", Kor. J. Chem. Eng. Vol. 28, 1882–1888, 2011.